Korean J. Chem. Eng., 36(12), 1983-1990 (2019)
DOI: 10.1007/s11814-019-0409-5

pISSN: 0256-1115
eISSN: 1975-7220

Effect of naphthalene quinoline and H_2S on DBT hydrodesulfurization over unsupported NiMoW catalyst

Changlong Yin†, Haonan Zhang, Tongtong Wu, Zhuyan Wu, Kunpeng Li, Yan Kong, Chengwu Dong, and Chenguang Liu

State Key Laboratory of Heavy Oil Processing, Key Laboratory of Catalysis, China National Petroleum Corporation (CNPC), China University of Petroleum, Qingdao, Shandong 266580, China
(*Received 24 June 2019 • accepted 15 October 2019*)

Abstract−Unsupported catalysts have attracted much attention for high activity in comparison with the traditional supported catalyst. Meanwhile, the clear structure of unsupported catalysts is helpful for the recognition of active phase for conducting the industry production. The NiMoW unsupported catalyst was prepared by hydrothermal synthesis and characterized by BET, XRD and HRTEM. The effects of naphthalene, quinoline and H_2S on the hydrodesulfurization reactivity of dibenzothiophene (DBT) were investigated in both a batch autoclave and a continuous 10 ml fixed bed micro-reactor over NiMoW and supported catalyst for comparison. The results showed that the hydrogenation reaction and the hydrogenolysis reaction occurred on different active sites. For supported catalyst, the inhibition was relatively weaker, and the inhibition of the hydrodesulfurization pathway was much higher than the direct desulfurization pathway. Although unsupported catalyst was very sensitive to quinoline and H_2S in this experiment, the HDS ratio on the unsupported catalyst was maintained at a high level above 99.7%, which is attributed to the very high active site density of unsupported catalysts.

Keywords: Unsupported Catalyst, Hydrodesulfurization, Naphthalene, Quinoline, H_2S

INTRODUCTION

Producing ultra-low sulfur diesel is the development trend of hydrodesulfurization (HDS). However, there are problems in the production process of ultra-low sulfur diesel. For instance, the sulfur in oil can inactivate the traditional catalyst, and aromatics (such as naphthalene, quinoline et al.) could also weaken the hydrodesulfurization activity. In-deep investigating reaction pathways of DBT over different catalysts and designing robust catalyst for deep hydrodesulfurization is of great significance [1-4]. Conventional hydrodesulfurization catalysts are supported catalysts where active component uniformly disperses on the support. The surface properties of the support and its interaction with metal active component can affect the dispersibility of the metal active site, but the catalytic activity is limited by metal content in supported catalysts. On the contrary, unsupported catalyst without support processes high content metal, large active site density and excellent hydrogenation performance in desulfurization [5], denitrification, and aromatic saturation reactions.

Diesel distillates contain components such as organic sulfide, nitride and polycyclic aromatic hydrocarbon, which affect the deep hydrodesulfurization reaction of DBT significantly, especially in aromatic-rich and nitride-rich diesels [6-10]. Only a small number of nitrogen-containing compounds can seriously affect the progress of the hydrodesulfurization reaction over supported catalyst. However, there are few studies on the effect of aromatics, nitrides and sulfides on hydrodesulfurization reaction over unsupported catalysts. Therefore, investigating the influence of aromatics, nitrides and sulfides on the hydrodesulfurization performance of DBT over unsupported catalysts to obtain suitable catalyst reaction conditions can provide guide for developing ultra-deep hydrodesulfurization catalysts.

Unsupported Ni/Co-Mo/W catalysts were studied because some properties of unsupported catalysts are magnified and the interference of the support is eliminated [11,12]. Therefore, unsupported catalyst is more suitable to observe the changes of active components to conduct specific research and provide theoretical support for industrial production. In this paper, NiMoW unsupported catalyst was prepared by hydrothermal synthesis. The effects of aromatics, nitrides and sulfides on DBT hydrodesulfurization over NiMoW catalyst were investigated using naphthalene, quinoline and H_2S as model compounds. NiMoW/Al_2O_3 supported catalyst was also studied for comparison.

EXPERIMENTAL

1. Preparation of Catalyst

1-1. Preparation of Unsupported Catalyst

The reagents used in the experiment were purchased from Sinopharm Chemical Reagent Company (PR China, Grade AR). The synthesis of the NiMoW catalyst has been described in detail before [13,14]. First, basic nickel carbonate ($NiCO_3{\cdot}2Ni(OH)_2{\cdot}4H_2O$), ammonium metatungstate ($(NH_4)_6W_7O_{24}{\cdot}6H_2O$), ammonium heptamolybdate ($(NH_4)_6Mo_7O_{24}{\cdot}4H_2O$) (the molar ratio Ni : Mo : W=

†To whom correspondence should be addressed.
E-mail: yincl@upc.edu.cn

2 : 1 : 1) and 150 ml of deionized water were placed in a beaker with a volume of 500 mL, the mixture was stirred. After shifting into an autoclave, the reaction was stirred at 90 °C for 10 h and a precipitate was obtained. Then, the precipitate was filtered by vacuum filtration and then dried for 10 h at 120 °C, the NiMoW catalyst precursor was obtained. Some nitric acid and distilled water (20 wt%) and alumina binder (70/30 by weight) were mixed with precursor. The product was extruded, dried at 120 °C for 10 h and calcined at 375 °C for 4 h. The NiMoW catalyst was obtained.

1-2. Preparation of $NiMoW/Al_2O_3$ Supported Catalyst

The equal volume impregnation method was employed to manufacture $NiMoW/Al_2O_3$ catalyst. The nickel nitrate, ammonium heptamolybdate and ammonium metatungstate were first dissolved in some water and the mixed solution was stirred at room temperature. Then, citric acid was added to the solution. The solution was impregnated into the alumina. The metal-impregnated catalyst was placed in an oven at 120 °C for 10 h, and then calcined at 375 °C for 4 h.

2. Catalyst Characterization

N2 adsorption-desorption experiments were carried out on a Micromeritics Tristar3000 (Quantachrome, USA) instrument. X-ray diffraction (XRD) characterization was performed on an X'Pert Pro MPD diffractometer using graphite-filtered Cu Kα radiation at a scan rate of 2 min^{-1} (Panalytical). The dispersion of the active components of the sulfided catalysts was investigated on a JEM-2100 (Japanese) microscope operated at 200 kV with EDS analysis (Oxford Instruments).

3. Catalytic Activity Evaluation

3-1. Evaluation of Catalyst Activity in Autoclave

The effect of aromatics, nitrides and sulfides on DBT hydrodesulfurization performance was tested in a FYX-0.5 autoclave. The catalysts were presulfided ex-situ on a continuous fixed bed reactor. 10 mL of 20-40 mesh catalyst particles were packed into the middle of the reaction tube, and the upper and lower ends of the reaction tube were filled with quartz sand of the same particle size. The cyclohexane solution containing 3 wt% of CS_2 was used as a presulfiding agent, and the presulfiding reaction was carried out at 330 °C for 8 h, a liquid hourly space velocity (LHSV) of 2.0 h^{-1}, a hydrogen pressure of 3 MPa, a H_2/oil ratio of 300. After sulfidation, the sulfided catalyst was cooled to room temperature and transferred into the autoclave under nitrogen protection, the reaction feed was a model compound of 2.0 wt% DBT in n-decane. 2.0 g catalyst was used and the catalyst to feedstock weight ratio was 1 : 100, the pressure was 5 MPa, and reaction temperature was 330 °C. The reaction product was analyzed by an Agilent gas chromatograph and GC-MS.

3-2. Evaluation of Catalyst Activity in Continuous Fixed Bed Microreactor

The effect of aromatics, nitrides and sulfides on DBT hydrodesulfurization was carried out on a 10 ml continuous fixed bed high pressure micro-reaction device. The 10 ml catalyst was presulfided in situ following the sulfidation steps described above. After sulfidation, four kinds of feeds containing different compounds in n-decane were pumped into the reactor alternately and the effects of nitrogen and aromatics on the performance of the catalyst were investigated by analyzing the product changes as model compound feed. The #1 feed was 2.0 wt% DBT, #2 feed was 2.0 wt% DBT and 5.0 wt% naphthalene, #3 feed was 2.0 wt% DBT and 1.0 wt% quinoline, #4 feed was 2.0 wt% DBT, 5.0 wt% naphthalene and 1.0 wt% quinoline. The reaction conditions were: total hydrogen pressure 4.0 MPa, LHSV 2.0 h^{-1}, H_2/oil ratio 300, temperature 280 °C. The feeding process was as follows: #1→#2→#1→#3→#1→#4 and samples were taken for GC analysis every two hours after switching the feed until the reaction was stable. The liquid phase product was analyzed by a GC214 gas chromatograph equipped with a 30 meter OV101 capillary column and a FID detector.

The deep hydrodesulfurization reaction network of DBT on unsupported catalyst is reported in detail in Refs. [6]. The cyclohexylbenzene, DBT hydrogenation product, can be further hydrogenated, generating hydrogenation pathway (HYD) in the DBT hydrogenation product, including cyclohexylbenzene (CHB), bicyclohexane (BCH), benzylcyclopentane (BCP), and cyclopentylcyclohexane (CPMCH). The sum of all these products is defined as CHB^+. The hydrogenolysis pathway (DDS) product is biphenyl (BP). The CHB^+/BP is used to represent the ratio of HYD and DDS pathways over unsupported catalyst.

RESULTS AND DISCUSSION

1. Catalyst Characterization

The compositions and BET surface results of the NiMoW and $NiMoW/Al_2O_3$ catalysts are shown in Table 1. The total metal content of the unsupported NiMoW catalyst was 80 wt%, and the supported $NiMoW/Al_2O_3$ catalyst was 30 wt%. The BET surface area of the unsupported NiMoW catalyst was higher than that of supported catalyst.

The XRD patterns of the oxide and sulfide catalysts are displayed in Fig. 1. Fig. 1(a) shows that the XRD pattern of NiMoW oxide catalyst was an amorphous phase of Ni-Mo-W complexes with 2θ peaks at 35.7°, 38.5°, 40.7° and 53.9° (JCPDS-card no: 50-1414) over unsupported catalyst and the phases of Al_2O_3 with 2θ peaks at 45.9° and 66.9° on supported catalyst, indicating the metal components are uniformly dispersed in the supported catalyst.

After sulfiding, the XRD patterns in Fig. 1(b) show the Ni_3S_2 structure with 2θ peaks at 21.9°, 31.2°, 37.9°, 44.5°, 50.2° and 55.3 (JCPDS-card no: 44-1418), and 2θ peaks at 14.4°, 33.5° and 58.9° corresponding to WS_2/MoS_2 structure (JCPDS-card no: 37-1492) in the sulfide unsupported catalyst. The WS_2/MoS_2 and Al_2O_3 peaks were detected on the supported catalyst.

Altamirano et al. [15] believed that MoS_2 and Ni_3S_2 are produced

Table 1. Compositions and properties of catalysts

Catalysts	MoO_3/wt%	WO_3/wt%	NiO/wt%	$S_{BET}/(m^2 \cdot g^{-1})$	$V_p/(cm^3 \cdot g^{-1})$	D_p/nm
NiMoW	20.4	32.6	27.0	241.0	0.32	5.6
$NiMoW/Al_2O_3$	7.6	12.2	10.2	130.2	0.31	9.2

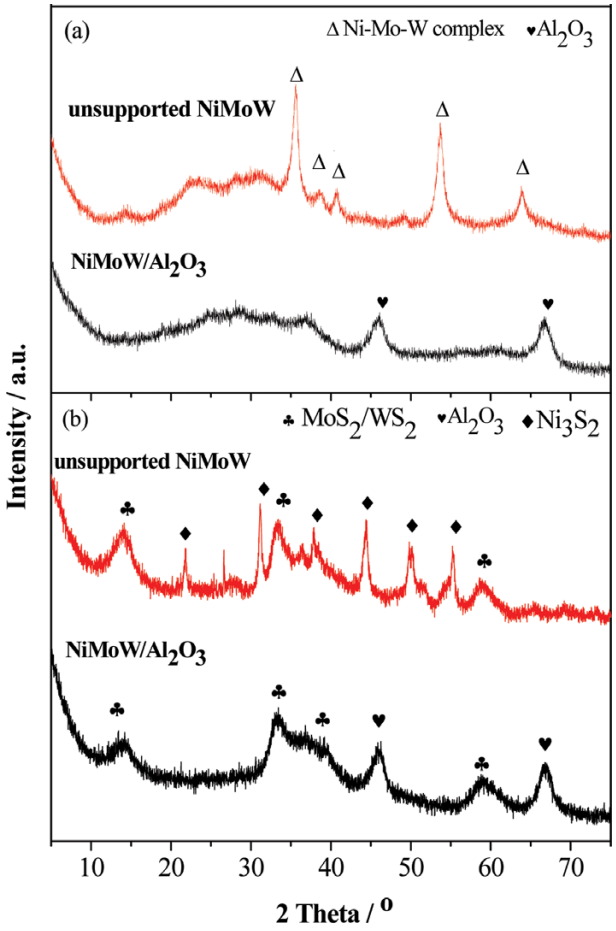

Fig. 1. XRD patterns of the oxidic (a) and sulfided catalysts (b).

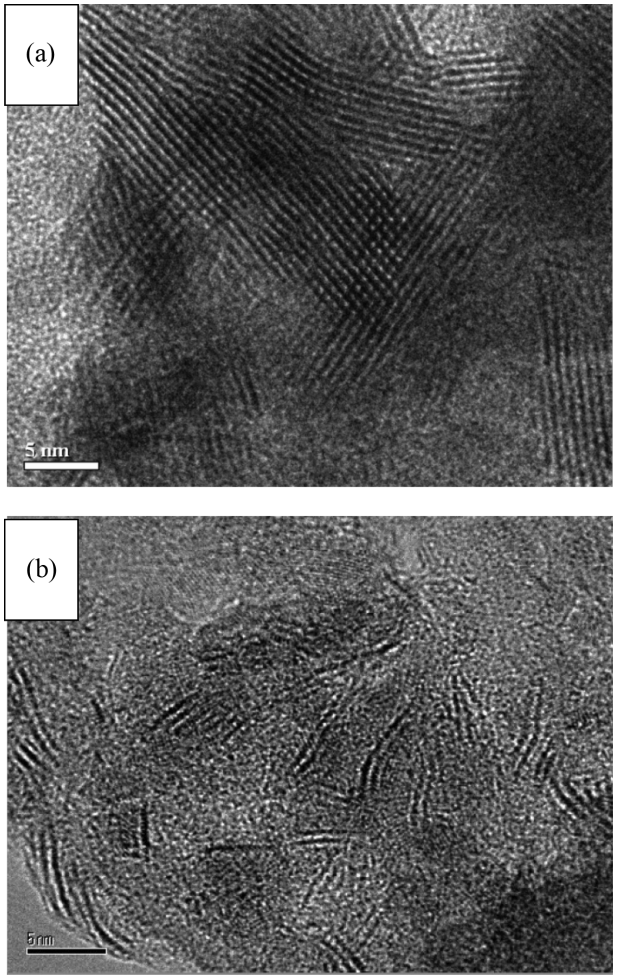

Fig. 2. The TEM images of sulfurized catalysts: (a) Unsupported, (b) supported.

by NiMoS active phase decomposition (NiMoS→Ni_3S_2+MoS_2). Therefore, the more MoS_2 and Ni_3S_2 were detected, indicating that the more NiMoS active phase was formed. Topsøe et al. [16] proposed that the NiMoS active phase is closely related to the catalytic activity of HDS catalysts. The unsupported catalyst exhibits more crystal phase structure of MoS_2 and Ni_3S_2, which is more favorable for HDS reaction.

The HRTEM images of the sulfided catalysts are exhibited in Fig. 2. Irregularly stacked layered structures were observed in the sulfided catalysts, which were attributed to the (002) basal planes of the MoS_2/WS_2 crystal phase structures [17], consistent with XRD

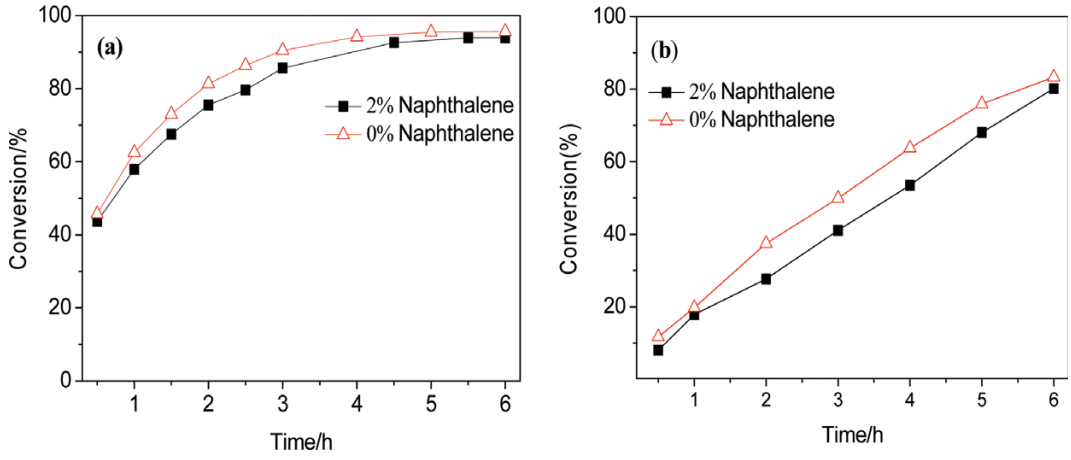

Fig. 3. Effect of naphthalene on the conversion of DBT on unsupported (a) and supported (b)catalysts.

results. Iwata et al. indicated that the active components of the sulfide catalyst are mainly located on the surface and the edge of the layer [18]. The unsupported catalyst exhibits more stacking layers, leading to more edge site and better contact between MoS_2/WS_2 and NiS to form NiMoS active phase, thus significantly promotes to HDS reaction.

2. Effect of Aromatics on DBT Hydrodesulfurization Reaction

Naphthalene is often used as a model compound to study aromatic hydrogenation in diesel oil. To investigate the effects of aromatics on the HDS of DBT, the following experiment was designed. The reaction was carried out in an autoclave, in which 2% naphthalene was added to the n-decane model compound of 3 wt% DBT. The conversion of DBT hydrodesulfurization reaction and the difference between HYD and DDS pathway (CHB^+/BP ratios in the product) on the supported and unsupported catalysts were compared. The results are shown in Fig. 3 and Fig. 4. It can be found that the DBT conversions and CHB^+/BP ratios of the unsupported catalyst are all higher than those of the supported catalyst. Naphthalene has no obvious inhibition on the conversion of DBT for supported and unsupported catalysts. However, it can be clearly seen from Fig. 4 that the inhibition effect of naphthalene on the CHB^+/BP of the unsupported catalyst is stronger than that of the supported catalyst. Farag et al. also found that the naphthalene increased the ratio of HYD/DDS in hydrodesulfurization of 4,6-Dimethyldibenzothiophene (4,6-DMDBT) over CoMo-Based Carbon Catalyst [19].

3. Effect of Nitrogen Compounds on DBT Hydrodesulfurization Reaction

The basic nitrogen compounds are considered to be stronger inhibitors of the HDS reaction than non-basic nitrogen compounds [20]. To investigate the inhibition of typical basic nitride (quinoline) to DBT hydrodesulfurization, 0.5% quinoline was added to the feed, and the results are presented in Fig. 5 and Fig. 6.

Quinoline has an obvious inhibition effect on the DBT hydrodesulfurization reaction. The inhibition of quinoline to HYD reaction is stronger than DDS, indicating that hydrogenation and hydrogenolysis occur in two different active sites of the catalyst. Nitride inhibition is achieved by adsorption of SP^2 lone pairs of electrons on the nitrogen atom. Fig. 5 shows that the addition of quinoline greatly inhibits the conversion of DBT on the unsupported catalyst, while the inhibition effect on the supported catalyst is relatively weak. The influence of quinoline on the ratio of CHB^+/BP is shown in Fig. 6, from which it could be found that the inhibition effect of quinoline on the HYD pathway was much higher than

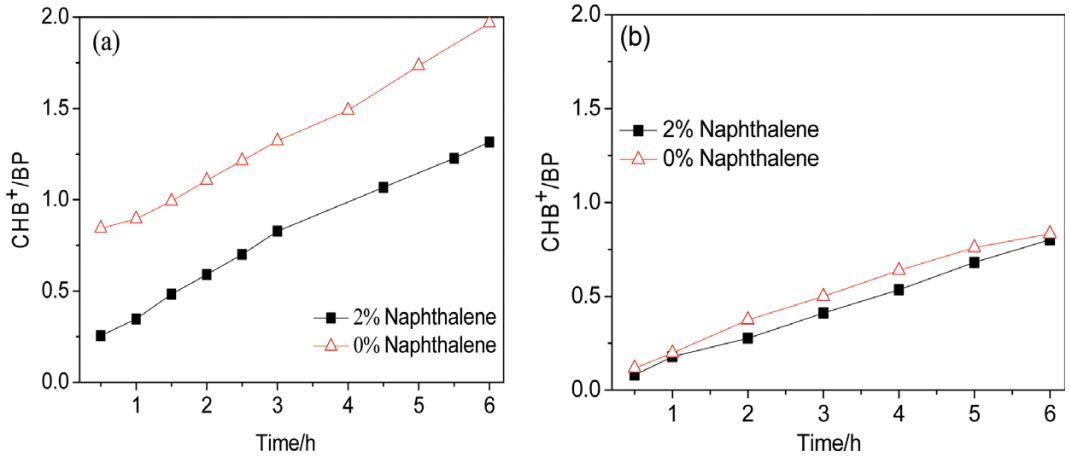

Fig. 4. Effect of naphthalene on CHB^+/BP of the products on unsupported (a) and supported (b) catalysts.

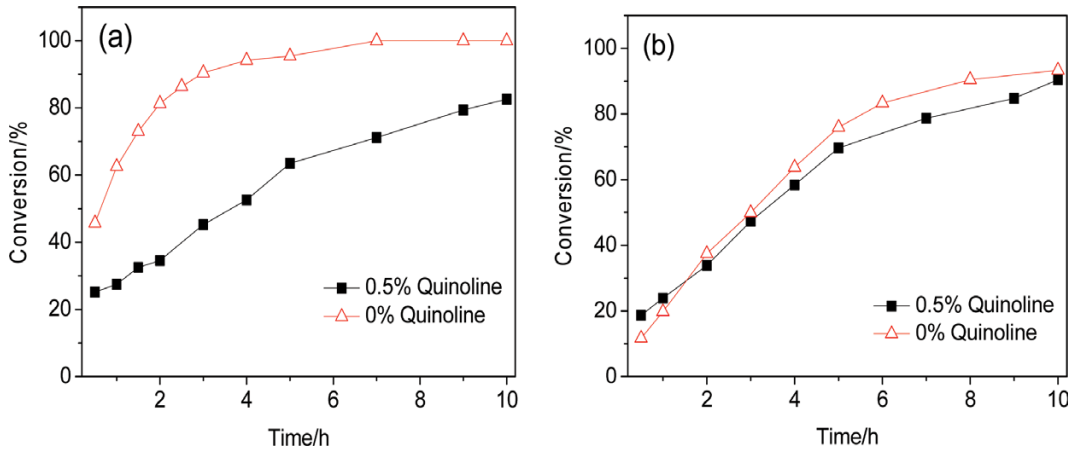

Fig. 5. Effect of quinoline on DBT conversion on unsupported (a) and supported (b) catalysts.

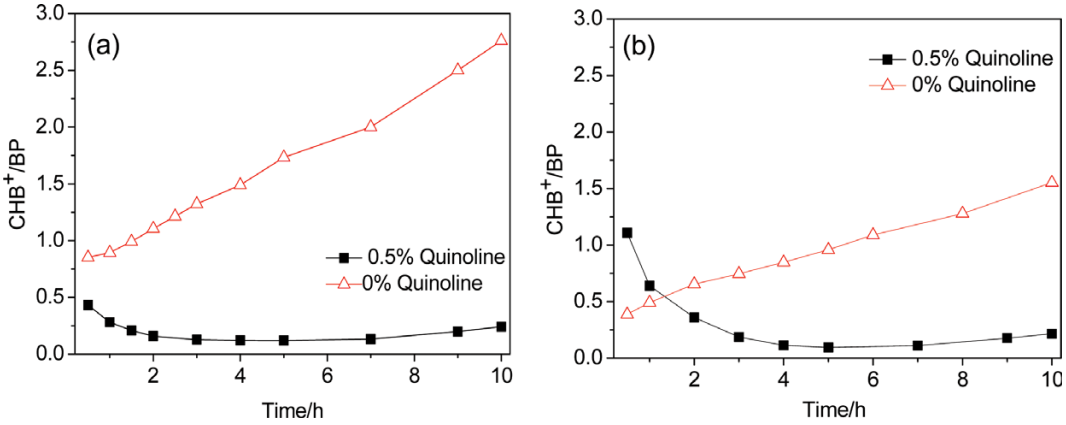

Fig. 6. Effect of quinoline on CHB^+/BP of the products on unsupported (a) and supported (b) catalysts.

that on the DDS pathway. The similar result for supported catalysts was also found in the literature [21].

4. Effect of Sulfides on DBT Hydrodesulfurization Reaction

Hydrogen sulfide is an important inhibitor for the ultra-deep desulfurization efficiency on the catalysts. Hydrogen sulfide is a product of hydrogenation of sulfur compounds in oil. To investigate the difference in the effect of sulfides on unsupported and supported catalysts, three levels of H_2S were generated in the DBT hydrodesulfurization reaction as the following three cases: (1) In situ H_2S was produced by DBT hydrodesulfurization; (2) CS_2 was added to the reaction system to generate additional 0.35% H_2S; (3) Enough copper was added to the reaction system to absorb the H_2S produced by the reaction (0%H_2S). The effects of H_2S on the DBT conversion and CHB^+/BP over different catalysts are shown

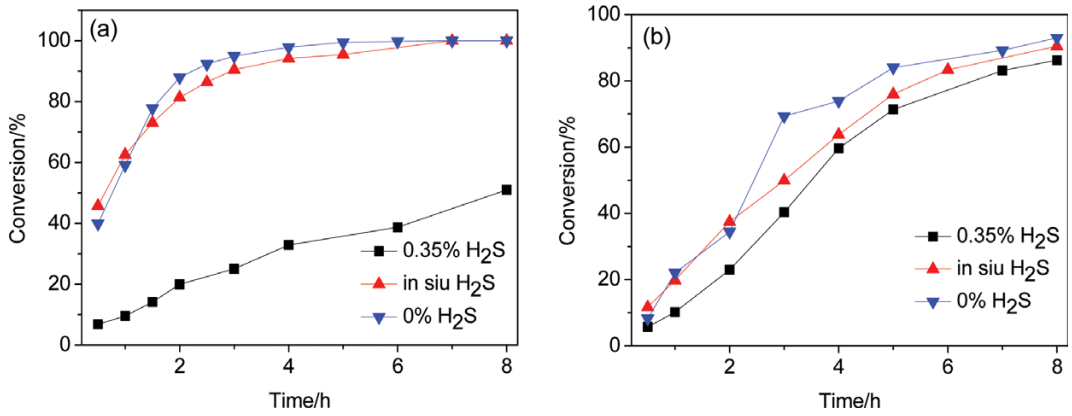

Fig. 7. Effect of H_2S on DBT conversion on unsupported (a) and supported (b) catalysts.

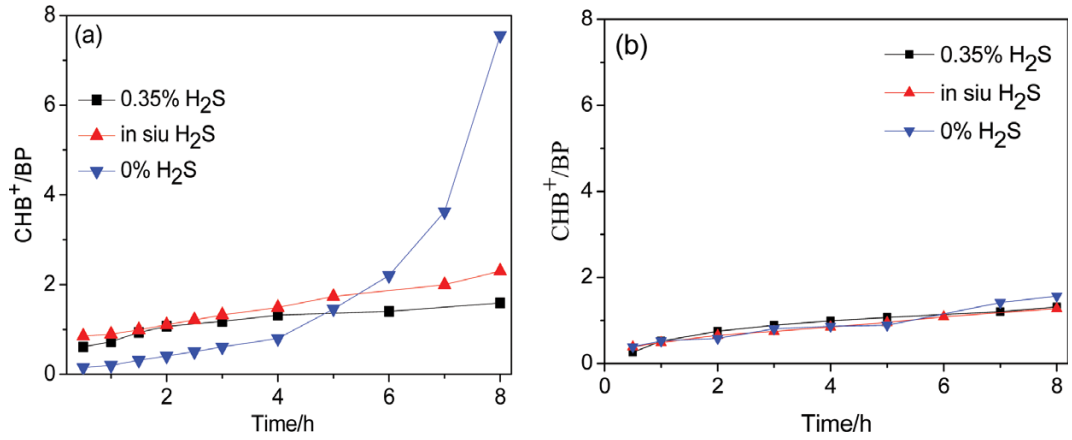

Fig. 8. Effect of H_2S on CHB^+/BP of the products on unsupported (a) and supported (b) catalysts.

in Fig. 7 and Fig. 8, respectively. The results show that the unsupported catalyst has higher hydrodesulfurization activity in the absence of H_2S and under *in-situ* H_2S conditions, while the desulfurization activity decreased significantly with additional 0.35% H_2S. Although the conversion of DBT desulfurization decreased with 0.35% H_2S addition, the inhibitory effects of H_2S on the hydrodesulfurization of supported catalyst are relatively invisible compared with unsupported catalyst.

It can be clearly seen from Fig. 8 that the inhibition of HYD pathway is stronger than DDS pathway of H_2S over unsupported catalyst. In the absence of H_2S, the CHB^+/BP ratio on the unsupported catalyst is about 7.5 finally, which is three-times higher than that in the presence of H_2S. This indicates that the inhibition of H_2S on the DBT hydrogenation pathway of the unsupported catalyst is significant. In contrast, the effects of H_2S on the DBT hydrodesulfurization of supported catalyst are slight. Kasahara et al. also found the HDS pathway of DBT was affected by H_2S over NiMo/$A1_2O_3$ catalyst [22].

5. Effects of Naphthalene and Quinoline on DBT Hydrodesulfurization in Continuous Fixed Bed Reactor

The effect of aromatics and nitrogen on the HDS reaction of DBT over the unsupported catalyst was investigated by continuous fixed bed reactor under four kinds of feeds containing different compounds in n-decane.

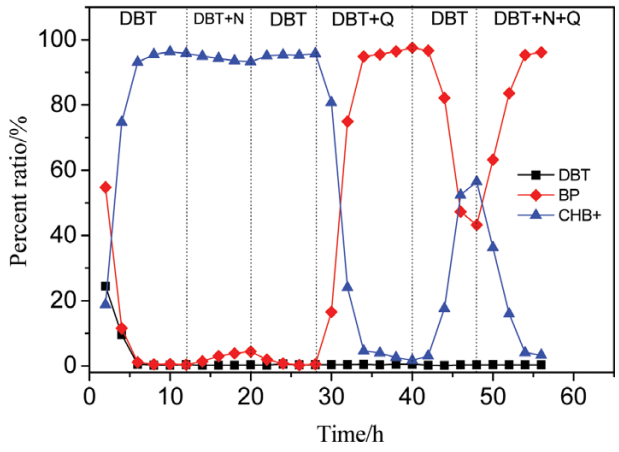

Fig. 9. The changes of DBT reaction product distribution on unsupported catalyst.

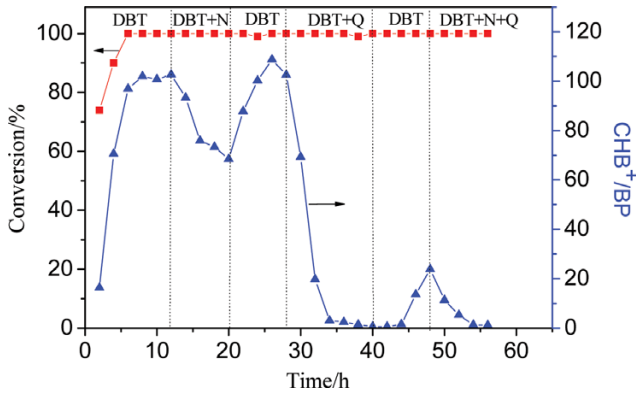

Fig. 10. The changes of DBT reaction product distribution, CHB/BP and DBT conversion on unsupported catalysts.

The product distribution of DBT, CHB^+/BP and DBT conversion on unsupported catalyst is shown in Fig. 9 and Fig. 10. After the naphthalene introduction, the amount of BP increased and the CHB^+ decreased slightly. After the DBT separately pumped, the amount of BP and CHB^+ was restored to the original level. After the quinoline introduction, the BP content increased and the CHB^+ content decreased. After the recovery of DBT alone, the amount of BP and CHB^+ rebounded, but far from the original level. It indicates that quinoline has irreversible effect on the corresponding hydrogenation active sites, and inhibitory the hydrodesulfurization of DBT on unsupported catalyst.

Naphthalene is easily adsorbed in the hydrogenation active site of the catalyst [23]. There is a competitive adsorption between Naphthalene and sulfides leading to a greater inhibitory effect on the depth of desulfurization reaction and increases the difficulty of desulfurization. Before the introduction of quinoline, the reaction pathway of DBT is dominated by the hydrogenation pathway. The introduction of quinoline has a great influence on the reaction pathway of DBT. The hydrogenation activity of DBT is inhibited, and the activity of hydrogenolysis is rapidly increased, which indicates that the hydrogenation reaction of the benzene ring and the hydrogenolysis reaction of the C-S bond occur at different active sites of catalyst. Prins et al. [24] also found this phenomenon when they studied the effects of 2-methylpyridine and 2-methylpiperidine on the hydrodesulfurization reaction of DBT. It is generally considered that Mo at the corner position of the MoS_2 crystal generates at least one sulfur hole adsorption reactant molecules [25-27]. Mo can be replaced by auxiliary Ni at the corner position to form the NiMoS phase [28], and the S atom with the Ni and Mo bonds can be easily removed to form holes. Therefore, the addition of an auxiliary agent can increase the activity of the Mo catalyst. The reaction of quinoline should start from the hydrogenation of benzene ring or pyridine ring. The hydrogenation active site of DBT is similar to that of quinoline, leading to competitive reaction. However, the lone pair electrons of the nitrogen atom on the quinoline molecule are not involved in the conjugation, so the pyridine ring electron cloud density of the quinoline is larger than the electron cloud density of the benzene ring of the DBT [23], and the quinoline preferentially adsorbed the DBT in the sulfur hole, which inhibits the hydrogenation reaction of DBT. After the quinoline is removed, a large amount of intermediate product remains on the catalyst, which has a continuous effect on the HDS reaction of DBT, making it difficult to restore the DBT reaction path to the original level. The result is basically consistent with the effects of quinoline on the DBT reaction on supported NiMo catalyst [29].

The rim-edge model proposed by Chianelli et al. [30] believes that MoS_2 has two active centers: rim-edge and edge, which correspond to the end edge and internal edge of MoS_2 particles, respectively. The rim-edge is related to hydrogenation activity, while the edge is related to hydrogenolysis activity. Therefore, DBT hydrodesulfurization has two paths: hydrogenation and hydrogenolysis. The hydrogenation pathway starts from the aromatic ring; the unsupported NiMoW catalyst has high aromatic ring hydrogenation activity due to it has more edges. In the experiment, CPMCH and

other products of DBT ultra-deep hydrodesulfurization were also found.

The typical hydrogenolysis pathway is listed as follows [31]. First, H_2 can be activated on S atom of catalyst edge to generate -SH. Then, hydrogen abstraction can occur between the adjacent -SH to generate gas H_2S and S hole, which can seize S atom of DBT, further leading to the broken of C-S bonds and the formation of biphenyl. The catalyst surface can be recovered with S atom retained on S hole, and integrated catalytic cycle is formed.

The high aromatic ring hydrogenation activity of the unsupported NiMoW catalyst is beneficial to the methyl-substituted aromatic ring hydrogenation. The alkyl-substituted dibenzothiophene compound can be removed more effectively. It is generally believed that the C-S bond cleavage in dibenzothiophene is carried out by eliminating the reaction mechanism [32]. S^{2-} acts as a basic site, the surface acidity of the catalyst is increased by the electron donating action of the active metal, thereby affecting the binding energy of the M-S bond and the electron density or pH of the surface of the catalyst S^{2-} [33,34], providing an active center for the fracture of C-S, which increases the activity of the hydrogenolysis pathway. The reason for the high hydrogenation activity is that the hydrogenation of one benzene ring causes heterotopy of the two benzene rings, reducing the steric hindrance.

The HDS ratio on the unsupported catalyst was maintained at a high level above 99.7%, and was no significantly inhibited by quinoline and naphthalene. This is mainly attributed to the much higher active site density of unsupported catalysts. When some active sites are inhibited by nitrides and aromatics, other active sites can exert higher hydrodesulfurization activity. Therefore, the unsupported catalyst can perform ultra-deep desulfurization of high-nitrogen high aromatic diesel and exhibit good adaptability to the reaction feed.

CONCLUSIONS

Naphthalene, quinoline and H_2S have inhibitory effects on the hydrodesulfurization of DBT. For unsupported catalysts, naphthalene had little effect on the reaction, while quinoline and H_2S made the reaction mainly dominated by hydrogenolysis pathway. For supported catalysts, naphthalene inhibited the hydrogenolysis pathway, quinoline and H_2S had relatively lower inhibition of hydrogenation pathway than unsupported catalysts. The effect of naphthalene on the distribution of the reaction product was quickly restored, and the effect of quinoline on the DBT reaction pathway was difficult to return to the original level. Although unsupported catalyst is very sensitive to quinoline and H_2S in this experiment, the HDS ratio on the unsupported catalyst has maintained at a high level, which attributes to the much high active site density of unsupported catalysts.

ACKNOWLEDGEMENTS

This work was financially supported by the National Natural Science Fund of China (Grant No. 21676301), the National key R & D program of China (2017YFB0602500). Financial support from the program of China Scholarships Council (No. 201806455007) and Petro China Corporation Limited is also greatly appreciated.

REFERENCES

1. J. Liang, M. Wu, P. Wei, J. Zhao, H. Huang, C. Li, Y. Lu, Y. Liu and C. Liu, *J. Catal.*, **358**, 155 (2018).
2. Y. Gao, W. Han, X. Long, H. Nie and D. Li, *Appl. Catal., B.*, **224**, 330 (2018).
3. T. Huang, J. Xu and Y. Fan, *Appl. Catal., B.*, **220**, 42 (2018).
4. D. Zhang, W. Q. Liu, Y. A. Liu, U. J. Etim, X. M. Liu and Z. F. Yan, *Chem. Eng. J.*, **330**, 706 (2017).
5. C. Liu, H. Liu, C. Yin, X. Zhao, B. Liu, X. Li, Y. Li and Y. Liu, *Fuel*, **154**, 88 (2015).
6. C. L. Yin, X. P. Zhai, L. Y. Zhao and C. G. Liu, *J. Fuel Chem. Technol.*, **41**, 991 (2013).
7. H. Wu, A. Duan, Z. Zhao, T. Li, R. Prins and X. Zhou, *J. Catal.*, 3**17**, 303 (2014).
8. W. Zhou, Q. Zhang, Y. Zhou, Q. Wei, L. Du, S. Ding, S. Jiang and Y. Zhang, *Catal. Today*, **305**, 171 (2018).
9. S. Ding, A. Li, S. Jiang, Y. Zhou, Q. Wei, W. Zhou, Y. Huang, Q. Yang and T. Fan, *Fuel*, **237**, 429 (2019).
10. F. Sánchez-Minero, J. Ramírez, A. Gutiérrez-Alejandre, C. Fernández-Vargas, P. Torres-Mancera and R. Cuevas-Garcia, *Catal. Today*, **133**, 267 (2008).
11. C. Yin, H. Liu, L. Zhao, B. Liu, S. Xue, N. Shen, Y. Liu, Y. Li and C. Liu, *Catal. Today*, **259**, 409 (2015).
12. A. Olivas, T. A. Zepeda, I. Villalpando and S. Fuentes, *Catal. Commun.*, **9**, 1317 (2008).
13. Y. Wang, C. Yin, X. Zhao and C. Liu, *Catal. Commun.*, **88**, 13 (2017).
14. C. Yin, Y. Wang, S. Xue, H. Liu, H. Li and C. Liu, *Fuel*, **175**, 13 (2016).
15. E. Altamirano, J. A. D. L. Reyes, F. Murrieta and M. Vrinat, *J. Catal.*, **235**, 403 (2005).
16. N. Y. Topsøe and H. Topsøe, *J. Catal.*, **84**, 386 (1983).
17. L. Wang, Y. Zhang, Y. Zhang, P. Liu, H. Han, M. Yang, Z. Jiang and C. Li, *Appl. Catal., A.*, **394**, 18 (2011).
18. Y. Iwata, K. Sato, T. Yoneda, Y. Miki, Y. Sugimoto, A. Nishijima and H. Shimada, *Catal. Today*, **45**, 353 (1998).
19. H. Farag, K. Sakanishi, I. Mochida and D. D. Whitehurst, *Energy Fuels*, **13**, 449 (1999).
20. H. Farag, M. Kishida and H. Al-Megren, *Appl. Catal., A.*, **469**, 173 (2014).
21. M. S. Nikul'Shina, A. V. Mozhaev, C. Lancelot, P. Blanchard, C. Lamonier and P. A. Nikul'Shin, *Russ. J. Appl. Chem.*, **92**, 105 (2019).
22. S. Kasahara, T. Shimizu and M. Yamada, *Catal. Today*, **35**, 59 (1997).
23. T. C. Ho, *J. Catal.*, **219**, 442 (2003).
24. M. Egorova and R. Prins, *J. Catal.*, **221**, 11 (2004).
25. J. Wan, Q. Liu, T. Wang, H. Yuan, P. Zhang and X. Gu, *Solid State Commun.*, **284**, 25 (2018).
26. K. C. Pratt, J. V. Sanders and V. Christov, *J. Catal.*, **124**, 416 (1990).
27. L. S. Byskov, J. K. Nørskov, B. S. Clausen and H. Topsøe, *J. Catal.*, **187**, 109 (1999).
28. P. Raybaud, J. Hafner, G. Kresse, S. Kasztelan and H. Toulhoat, *J. Catal.*, **190**, 128 (2000).
29. C. E. Xiang, Y. M. Chai, J. Fan and C. G. Liu, *J. Fuel Chem. Technol.*, **39**, 355 (2011).
30. R. R. Chianelli, M. Daage and M. J. Ledoux, *Adv. Catal.*, **40**, 177

(1994).
31. W. H. Qian, A. Ishihara, Y. Okoshi, W. Nakakami, M. Godo and T. Kabe, *J. Chem. Soc. Faraday Trans*., **93**, 4395 (1997).
32. F. Bataille, J. L. Lemberton, P. Michaud, G. Pérot, M. Vrinat, M. Lemaire, E. Schulz, M. Breysse and S. Kasztelan, *J. Catal*., **191**, 409 (2000).
33. R. R. Chianelli, G. Berhault, P. Raybaud, S. Kasztelan, J. Hafner and H. Toulhoat, *Appl. Catal., A*., **227**, 83 (2002).
34. M.-T. Nguyen, M. Tayakout-Fayolle, F. Chainet, G. D. Pirngruber and C. Geantet, *Appl. Catal., A*., **530**, 132 (2017).